PERGAMON

Electrochimica Acta 46 (2001) 3351–3358

ELECTROCHIMICA Acta

www.elsevier.com/locate/electacta

Transference number measurements of TiO_2–BaO melts by stepped-potential chronoamperometry

Naomi A. Fried, Kevin G. Rhoads [1], Donald R. Sadoway *

Department of Materials Science and Engineering, Massachusetts Institute of Technology, Cambridge, MA 02139-4307, USA

Received 20 November 2000; received in revised form 30 March 2001

Abstract

TiO_2–BaO melts have been under investigation as candidate electrolytes for the electrolytic production of titanium. Transference number measurements have been made by stepped-potential chronoamperometry at two compositions: 67 mol% TiO_2 ($1328 < T < 1487$°C) and 73 mol% TiO_2 ($1210 < T < 1477$°C). A theoretical analysis of the technique, capable of distinguishing between variations in ion density and variations in net free-charge density, is presented.

Keywords: Transference number; Chronoamperometry; Molten salts; Titanium; Barium oxide

1. Introduction

Accurate knowledge of the electrical properties of molten salts is paramount in the design of industrial electrolytic cells because joule heating of the electrolyte is central to establishing the thermal balance of the reactor. Molten oxides have been named candidate electrolytes for prospective high-temperature electrochemical processes [1]. In particular, Sadoway has speculated on the utility of producing titanium metal by direct electrolytic reduction of TiO_2 dissolved in a suitable oxide solvent [2]. With conductivities exceeding 70 S/cm molten titanates are known to be liquid semiconductors [3,4] and therefore must be modified in order to be useful as industrial electrolytes. The purpose of the present study was to determine to what extent electronic conduction would be reduced by dissolving TiO_2 in a solvent that is predominantly ionic. BaO was chosen because barium is electrochemically more reactive than titanium and therefore, in principle, it should be possible to reduce titanium electrochemically from such a melt. In parallel, there is evidence in systems such as TiO_2–MgO and TiO_2–CaO that at high concentrations of alkaline-earth oxide the conductivity drops to values typical of ionic melts [5,6]. Transference number measurements were made in TiO_2–BaO melts by stepped-potential chronoamperometry, a technique that has been widely used in the past. Here we present the results from the molten barium titanate solutions and provide a theoretical analysis of the technique itself. Unlike previous treatments, ours is capable of distinguishing between variations in ion density and variations in net free-charge density.

2. Background

By direct comparison of measurements made by different techniques, Olsen et al. conclude that the dc polarization technique, stepped-potential chronoamperometry, is as effective as the Hittorf (Turbandt), NMR or radiotracer, and concentration cell methods for measuring transference numbers [7]. Stepped-potential chronoamperometry has been used to measure the elec-

* Corresponding author.

E-mail address: dsadoway@mit.edu (D.R. Sadoway).

[1] Present address: Varian Semiconductor Equipment Associates, Newburyport, MA 01950, USA.

0013-4686/01/$ - see front matter
PII: S0013-4686(01)00531-X

trical properties of polymers [8–10], solid oxide electrolytes [11], and mixed oxide conductors such as $Li(Na)_xMo_2O_x$ [12]. Furthermore, to obtain information about the specimen's charge carriers one can monitor either the voltage decay or the current decay[2] as a function of time [13]. Colson et al. modeled the choke-off of the ionic current by a resistor–capacitor model using double-layer charging [12]. This kind of model, while attractive for its simplicity, cannot explain the long observed time scales of ionic current choke-off without assuming physically unrealistic values for various physical parameters, e.g. double-layer capacitances. In effect, dc polarization is a technique that has proven to be reliable and accurate, but for which a theoretical model is lacking. In the course of measuring transference numbers in TiO_2–BaO melts, we attempted to model the dynamics of the technique by viewing it from an atomistic viewpoint. To our surprise, we found a model that is applicable to a wide range of systems and that explains and justifies square wave chronoamperometry as a method of determining transference numbers, provided only that certain rather reasonable conditions are satisfied.

3. Theory

3.1. System definitions

We consider a system of mixed conduction, having at least one mobile ionic carrier and at least one mode of electronic conduction. When specifics are needed for examples, we will use Ba^{2+} as the mobile ion and polaron hopping between TiO_x^{n-} complexes as the mode of electronic conduction. We shall further extend the model to treat situations in which there is a plurality of mobile ionic species and a plurality of modes of electronic conduction.

The system is defined to include the bulk melt, but to specifically exclude bounding double layers. During transients, there will be dynamics from charge transport in the bulk, and these are the central focus of the model. Excluded from the model are dynamics from such things as electrode processes, the double layers, and external circuit elements.

3.2. The hierarchy of time scales

To help keep track of the various operative kinetic processes we recognize a hierarchy of time scales. Since the ideal excitation for the square wave technique is a square pulse of voltage, one of the shortest time scales is the rise time of applied potential. This time is set by the external instrumentation and certain electrical properties of the system, such as total resistance and capacitance, as well as cable inductances. Another short time scale is the time to charge the double layer. In contrast, the time scale of interest in the measurement is longer, ranging from seconds to hours, and is dominated by charge transport dynamics in the bulk. On this time scale we have dynamics resulting from the division of current amongst ohmic and diffusional transport processes, and the dynamics of the evolution of ion number density profiles throughout the bulk. A final time constant of interest is that of dielectric relaxation in the bulk, and this time constant is typically the shortest of all, which leads to some very useful simplifying approximations.

An experiment to determine transference numbers begins with a system that has been equilibrated for a long time with no applied potential. Then the electrodes are polarized so as to set the potential at a value different from the rest potential, and the double layers charge. These transients attenuate in a matter of microseconds to milliseconds. At this point in time, denoted $t = 0^+$, our model begins. Although, strictly speaking, it takes time to charge the double layers, if the external instrumentation driving the system is of low enough impedance, the time to do so is 'very short,'[3] and therefore conditions in the bulk are in all respects but one the same as they were prior to the application of voltage. The sole difference is the presence of an electric field. However, the number densities of all species remain homogenous and, as we show rigorously later, there is no net free-charge accumulation anywhere in the bulk. At $t = 0^+$ only the double layers have had chance to react to the applied potential, and the transients associated with their charging have progressed close enough to their asymptotic limits as to be negligible.

3.3. Quasi-neutrality and the Imposed Field Model

In general, there is a synergistic relationship between charge transport and the applied electric field: each can affect the other. However, there are some rather commonly used special-case approximations for situations in which the field remains unchanged by charge transport. We demonstrate that one such approximation, the imposed field model based upon an assumption of quasi-neutrality, is valid for our systems.

[2] In the melt, current and potential are related through Ohm's law ($V = iR$). For this work, current was easier to measure, and its decay was monitored.

[3] The value of the specific double-layer capacitance in molten oxides has been measured by Esin et al. to be about 2000 μF/cm^2 [14]. With our electrode geometries, this gives a double-layer capacitance of about 500 μF. Likewise, taking the electrical conductivity of the melt to be about 50 S/cm [3,4] gives a bulk resistance of about 0.01 Ω [15]. Thus, we estimate a time constant for double-layer charging to be $\tau = RC = 5$ μs.

Consider only two processes in the bulk: ohmic conduction and dielectric polarization, and the interaction between them. This interaction is typically called charge relaxation and is governed by a single time constant for any single bulk region. For materials of high ohmic conductivity, the time constant is extremely short. This implies both quasi-neutrality and an imposed electric field.

Dielectric polarization is related to free charge by Gauss's equation for charge, which connects the divergence of displacement flux density, D, to net free charge, ρ_{free}

$$\nabla \cdot D = \rho_{\text{free}} \tag{1}$$

while ohmic conduction is related to the time rate of change of free charge through charge conservation, which connects the divergence of current density, J, to the time partial derivative of net free charge

$$\nabla \cdot J = -\partial \delta \rho / \partial \delta t \tag{2}$$

For linear dielectric materials, the constitutive relation between displacement flux density and electric field is

$$D = \varepsilon E \tag{3}$$

Similarly, for current density in ohmic conductors

$$J = \sigma E \tag{4}$$

Combining these equations leads to a simple first-order, linear differential equation for free charge density in a homogenous ohmic, linear dielectric

$$\partial \delta \rho / \partial \delta t = -\rho_{\text{free}} / (\varepsilon / \sigma) \tag{5}$$

Given any initial free charge distribution, i.e. at some designated time $t = 0$, $\rho(r, 0)$, we can determine the free charge density at any later time by

$$\rho(r, t) = \rho(r, 0) \exp(-t/\tau) \tag{6}$$

where $\tau = \varepsilon / \sigma$.

Thus, in any system with high ohmic conductivity, any initially present net charge will decay with a time constant of ε over σ. For anything even moderately conductive this time scale is very short. For molten salts and molten oxides with multivalent ions this time scale will typically be of the order of nanoseconds or even picoseconds. For the $BaO–TiO_2$ system we were specifically investigating, a conservative (i.e. highly inflated) estimate was 5×10^{-12} s over the temperature range of the investigation. Clearly for experiments occurring over time scales of minutes and resolving time to milliseconds, net charge in the bulk is not an issue.

This approximation is dependent upon a sufficiently large ohmic conductivity of the material being investigated. This is the first requisite condition for this model: that the system be conductive enough that the assumption of quasi-neutrality and imposed field be a good approximation. An easy way to test the validity of this approximation is to compare the time constant of dielectric relaxation to the time scale of interest.

The implications of this approximation are that material in the bulk will become and remain uncharged. Barium ions are present, but their charge is screened by an equal and opposite charge distributed amongst the TiO_x^{n-} complexes. Even in the presence of other dynamics that attempt to accumulate net free charge in the bulk, dielectric relaxation is so fast and so complete that the charge is neutralized as it tries to accumulate. As a result, electric-field dynamics are decoupled from charge-transport dynamics. The electric field and potential can be solved using Laplace's equation with values of potential imposed at the boundaries and remain constant throughout the evolution of charge-transport dynamics.

3.4. Charge-transport atomistics

We model an ionic conductor in which there is only one mobile ionic species. In the specific system we studied, the mobile species is barium, Ba^{2+}; there is no free oxide, O^{2-}: rather, oxygen is present in the form of polyatomic titanate complexes of varying stoichiometry and charge, TiO_x^{n-}. The mobilities of the titanates are lower than that of the barium ions. More important, polaron hopping from titanate to titanate is so facile, that charge transport due to motion of titanate complexes is negligible. In response to local electric fields, before a titanate can move appreciably, it will gain or lose an electron by polaron hopping. Hence, there are three charge-transport processes to consider: barium ion diffusion, barium ion drift, and electron drift. The net effect of all drift modes is expressed by the total ohmic conductivity. Electron diffusion is not considered because there is no electron solvation in titanate melts, i.e. there are no free electrons: only electrons localized on titanate complexes.

To relate charge-transport atomistics to continuum variables, we have the following. From Fick's first law, the barium ion diffusion current, $J_{\text{Ba diffusion}}$, is related to the gradient of the barium ion number density, N_{Ba}, by[4]

$$J_{\text{Ba diffusion}} = -z_{\text{Ba}} e D_{\text{Ba}} \nabla N_{\text{Ba}} \tag{7}$$

The total current is

$$J = \sigma_{\text{e}} E + \sigma_{\text{Ba}} E - z_{\text{Ba}} e D_{\text{Ba}} \nabla N_{\text{Ba}} \tag{8}$$

Clearly, to evaluate the current by Eq. (8) one needs to know the spatial variation of the barium number density. There are two special cases where this can be

[4] For convenience, in the subscripts, Ba^{2+} will be denoted as simply Ba.

expressed in analytic closed form. In general, both the barium number density and the current density are dependent upon both time and position, and the expressions for each are highly dependent upon the details of instant electrode geometry. For the two special cases, however, things are much simpler.

3.5. Case I, $t = 0^+$

As has been described, the experiment begins with a long equilibration time at zero applied potential. During this time the ion concentrations will relax to uniformity outside the double layers. So for this $t = 0^+$ case, N_{Ba} is not a function of position. Thus, its gradient is zero. Accordingly, the current is solely ohmic:

$$J = \sigma_e E + \sigma_{Ba} E \tag{9}$$

3.6. Case II, $t \to \infty$

In the long-time limit, the barium number density is no longer uniform; however, its spatial variation is readily determinable. Since the square-wave technique uses applied potentials that are well below the decomposition potentials of any species present in the electrolyte, no faradaic reactions can occur at the electrodes; thus, no ion can be added to or removed from the system. Hence, the barium ions drift in response to the applied electric field, but they cannot exit the system. In the long-time limit, the net barium flux must be zero. This happens because, for barium, diffusion exactly balances drift:

$$J_{Ba} = \sigma_{Ba} E - z_{Ba} e D_{Ba} \nabla N_{Ba} \to 0 \tag{10}$$

We prove, by construction, that such a barium ion number density exists. This proof is accomplished by relating barium concentration back to electric potential. Since the conditions are long established under which Laplace's equation guarantees the existence and uniqueness of a solution, relating the existence and uniqueness of the necessary solution for the barium ion concentration to the solution of Laplace's equation allows us a rigorous proof without the necessity of using partial differential equations.

Setting $J_{Ba} = 0$ in the long-time limit, we simplify the expression by expanding the ohmic conductivity $\sigma_{Ba} = \mu_{Ba} z_{Ba} e N_{Ba}$ and exploiting the Einstein relation, $D_{Ba} = \mu_{Ba}(kT/e)$, so that Eq. (10) becomes

$$\mu_{Ba} z_{Ba} e N_{Ba} E - z_{Ba} e \mu_{Ba} (kT/e) \nabla N_{Ba} = 0 \tag{11}$$

which simplifies to

$$N_{Ba} E - (kT/e) \nabla N_{Ba} = 0 \tag{12}$$

Since we are operating in conditions where the imposed field approximation is valid, we take E as a known and constant quantity, which is the negative gradient of electric potential. Rewriting to exploit this we have

$$\nabla N_{Ba}/N_{Ba} = \nabla \ln(N_{Ba}) = E/(kT/e) = -\nabla \Phi/(kT/e) \tag{13}$$

A completely general expression for the number distribution can be found by taking the line integral[5] of Eq. (13) from $r = r_o$ to r.

$$\int_{r=r_o}^{r} \nabla N_{Ba}/N_{Ba} \cdot \mathrm{d}l = (-e/kT) \int_{r=r_o}^{r} \nabla \Phi \cdot \mathrm{d}l \tag{14}$$

Integrating and exponentiating give the expression for the number density of N_{Ba} in the long term limit as a function of a constant $N_{Ba}(r_o)$ and the potential, Φ:

$$N_{Ba}(r) = N_{Ba}(r_o) \mathrm{e}^{-(\Phi(r)/V_{th})} \tag{15}$$

where $V_{th} = kT/e$.

The value of the constant $N_{Ba}(r_o)$ is evaluated by applying the law of conservation to barium ions and equating the volume integral of the number distribution of barium at $t = 0^+$ and $t \to \infty$.

It should be recognized that the difficulty of solving partial differential equations has not really been avoided; rather, the difficulty of finding the long time limit for N_{Ba} has been surmounted by finding the potential, Φ. However, the principle of reducing a new problem to one previously solved has a long and honorable history in mathematics and the sciences, and we are humbly grateful that we can so exploit it here.

In the long time limit with this distribution of barium ions the barium current density and flux are everywhere zero throughout the volume. Since these two components of the total current sum to zero, the sole remaining term is the total current:

$$J = \sigma_e E \tag{16}$$

3.7. Conclusions about transference number measurements

Thus it is proven that, given the conditions necessary for the simplifying assumptions used, in the two limiting cases the current density can be simply derived. Furthermore, in the short time limit, the net current density is ohmic with both electronic and ionic contributions, whereas in the long time limit the net current density is again ohmic, but with only the electronic contribution. Since the external circuit currents are found simply from the integrals of the current density over the appropriate surfaces, the transference ratio can be determined from the total currents as well as the current densities, provided only that the cell constant does not change over the course of the experiment. The

[5] The integral is simplified if the boundaries are set such that $\Phi(r_o) = 0$.

instant value of the cell constant need not be determined; furthermore, over the longer term it is not imperative that the cell constant remain unchanged. In fact, the only requirement on the cell constant is that for any pair of measurements it remain constant over the time interval spanning the first measurement at $t = 0^+$ and last measurement at $t \to \infty$. Accordingly, the cell constant can change between one pair of measurements and the next, as is likely when a series of measurements is made at different temperatures. Therefore, since the constraints on the cell constant are so relaxed, it is possible to obtain high-accuracy transference measurements under conditions wherein accurate determination of conductivity would be impossible.[6]

3.8. Extension to systems containing a plurality of mobile ions

Although the derivation above considered a system containing a single mobile ion, the treatment can be trivially extended to handle a plurality of mobile ions, provided such ions are neither created nor destroyed, i.e., the experiment is conducted with blocking electrodes (no faradaic processes). This extensibility is another consequence of quasi-neutrality. The dynamics of charge transport in the bulk have no effect upon the electric field distribution, so there is no coupling among charge transport dynamics of separate species. Each species will evolve independently and achieve the ion density distribution required for diffusion to balance drift.

3.9. Extension to systems having a plurality of modes of electronic conduction

The derivation above considered a system with a single mode of electronic conduction, polaron hopping. However, the presence of multiple modes of electronic conduction is easily managed by simply summing the contributions of all such modes into a total electronic conductivity.

3.10. The finite time transient

With the knowledge of the expressions for ion number density distributions at the two temporal extremes, $t = 0^+$ and $t \to \infty$, the general solution was examined to see if it could be simply expressed in terms of these limiting solutions. We found that the finite-time solution is governed by a form of the diffusion equation, enhanced to include drift terms. The finite-time solution is highly dependent upon the details of the instant geometry. Just the same, certain conclusions can be drawn without fully deriving the solution, and which are thus applicable to all cases.

3.11. Many time constants

The most relevant of these conclusions is that there will be an infinite number of time constants for the decay of the transient. Unlike a single resistance-capacitance circuit, which has a single time constant, the solution of a time dependent diffusion equation is expressed in modes specific to the geometry, and each mode has its own time constant. Typically in a Fourier, Fourier–Bessel, or similar modal expansion, an infinite number of modes is required. As a result, there will typically be an infinite number of time constants. Any attempt to fit the decay to a single time constant will be an approximation yielding, at best, the value of the longest time constant.

A derivation of the relationships between these time constants can be obtained for certain particularly simple geometries, such as parallel plate or coaxial cylinder. However, undertaking such an analysis for the kinds of geometries typically found in experimental conductance cells requires sophisticated numerical analysis, which yields meaningful results only for that specific geometry. Furthermore, this provides no great insight into the mechanism by which transference determination is accomplished. So beyond noting the presence of an infinite number of time constants in the transient solution, we let the matter rest.

4. Experimental

The electrical properties of two melts in the barium titanate system were measured as a function of temperature. This system was chosen because of all the candidate supporting electrolyte solvents for TiO_2, the TiO_2–BaO binary has the twin attributes of a deep eutectic (~ 1312°C) [15] and low vapor pressure.[7]

In an argon-filled glove box, proper quantities of BaO (99.5%, < 100 mesh, packed under argon, Cerac) and TiO_2 (99.9%, < 325 mesh, packed under argon, Cerac), along with a constant 1 weight per cent of MoO_2 (99%, Alfa, Ward Hill, MA) to fix the partial

[6] For a specification of conditions for making highly accurate conductivity measurements, the reader is directed to [16].

[7] No direct evidence here; however, the vapor pressures of the pure components are low and due to complex formation it is expected that the binary solutions in the vicinity of the eutectic will be even less volatile.

pressure of oxygen[8] were weighed, combined, and vigorously shaken. The mixture was then charged into the reactor tube which was then capped. Under vacuum the powders were heated at a rate of 250 K/h to 500°C and held at this temperature for a minimum of 4 h. The reactor was then backfilled with ultra-high purity (UHP) argon and heated at a rate of 250 K/h to 1450°C under flowing argon. After 1 h the melt was allowed to cool to room temperature. Back in the glove box the reactor was fitted with a second cap which held the electrodes and thermocouple.

Measurements were made in a four-electrode cell. The crucible and a central rod mounted coaxially served as injecting electrodes. Placed between these were two more rods which served as sensing electrodes. The crucible was a right-circular cylinder machined of molybdenum (Phillips Elmet, Lewiston, ME), 8 in. tall, 1.5 in. i.d., and wall thickness 0.06 in. A solid molybdenum rod, 18 in. long, 1/8 in. in diameter, served as the lead to the crucible. The two were connected by a mechanical arrangement involving molybdenum wire threaded through holes in the top of the crucible and holes in the rod. The three other electrodes were solid molybdenum rods, 18 in. long. The central electrode was 1/8 in. in diameter, while the sensing electrodes were 1/16 in. in diameter. Temperature was measured by a molybdenum-sheathed ASTM type-R thermocouple immersed in the melt. An Omega DP-41 temperature indicator (Omega Corporation, Stamford, CT) with built-in electronic ice-point converted the Seebeck voltage into temperature. Within the reactor tube alignment of the electrodes and thermocouple was assured by a spacer machined of hot-pressed boron nitride sitting on the top of the crucible and suspended from a molybdenum rod. To prevent shorting, the electrodes were electrically isolated from the metal cap by a layer of FEP shrink tubing (Tex-Loc, Ft. Worth, TX).

A 2.0-in. i.d. stainless steel Kwik Disconnect Cap (Huntington, Mountain View, CA) was fitted with a customized top plate. Welded to this top plate were several Cajon Ultra-Torr (Cambridge Valve and Fitting, Billerica, MA) compression fittings with viton o-rings which served as feedthroughs for the electrodes, thermocouple, and spacer holder. The Kwik Disconnect Cap was further customized by welding stainless steel tubing to two holes machined on opposite sides. The tubing was connected by Swagelok fittings to two Nupro vacuum valves with a soft seat (B-4HK, Cambridge Valve and Fitting, Billerica, MA). One valve provided an inlet for argon. The other was connected to the vacuum manifold which allowed release of pressure to a vacuum pump or through a bubbler to house vacuum. The Kwik Disconnect Cap used a compression fitting with 226 viton o-ring and ferrule to attach to the 2.0-in. o.d. (1.75-in. i.d.) 15-in.-long round-bottom 99.8% alumina reactor tube (Vesuvius McDanel, Beaver Falls, PA). To prevent the crucible from tilting inside the round-bottom reactor tube a 0.25-in. thick, 1.6-in. diameter alumina disk was used as a platform at the bottom of the reactor tube. One-in. wide ceramic tape (Zircar, Florida, NY) was wound around the reactor tube below the cap and tied down with chromel wire to produce a 1-in. thick heat plug.

A vertical tube furnace with a 2.0-in. bore, built and designed in house, provided the heat for these experiments. Six silicon carbide heating elements (SE $18 \times 9 \times 0.5$ I Squared R, Akron, NY) were arranged in a delta configuration. A three-phase, 208-V, S.C.R. power controller (Omega Model SCR73, Stamford, CT) was used with a programmable p.i.d. temperature controller (Omega CN2011, Stamford, CT) connected to a type-R thermocouple to tune and control the furnace. When properly tuned, the furnace was capable of holding temperature within ± 0.5°C in the hot zone. An alumina, closed-one-end, round-bottom furnace tube with a 2-inch i.d. was the receptacle for the reactor tube. The metallic case of the furnace was grounded. To keep the cap cool enough to prevent decomposition of the o-rings, two sheets of ceramic fiber insulation were placed on top of the furnace and a set of four fans was positioned about the reactor cap where it extended above the furnace.

The measurement of small electrical signals is highly sensitive to noise on the electrical line; accordingly, our instrumentation was protected by isolation power transformers to ensure that the line power was uncorrupted by local network noise. Noise was further decreased by the placement of a metal stool on the top of the furnace. The metal stool provided a conducting ring about 4 in. above the furnace at the height of the electrical connections to the cap. This decreased the noise from stray magnetic fields. The legs and top plate formed additional conducting rings effective at shielding random magnetic fields. The furnace and, therefore, the stool were grounded through connection with the ground wire of the power line. The seat of the stool acted as a shield against incoming electric fields.

Measurements were made by a potentiostat (Solartron 1286 Electrochemical Interface, Solartron Instruments, Allentown, PA) which applied a voltage between the crucible electrode and the center rod electrode and measured the current response. The instrument was controlled by a personal computer running CorrWare (Scribner Associates, Inc., Southern Pines, NC). A four-channel digitizing oscilloscope (Tektronix 420A, Wilsonville, OR) was used to record the applied voltage, melt current, and melt voltage, and to provide

[8] The electrical properties of certain semiconducting oxides are influenced by the partial pressure of oxygen. To set the oxygen potential in the melt, a small amount of MoO_2 was added. This would, in turn, equilibrate with metallic molybdenum in the crucible and thermocouple sheath.

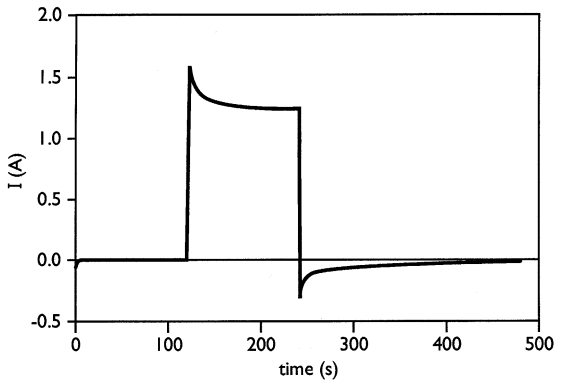

Fig. 1. Current response to square-wave voltage excitation. TiO_2–BaO (73 mol% TiO_2). $T = 1400$°C. Potential step = 80 mV. Initial current peak of 1.62 A decaying to 1.27 A. Initial relaxation peak of -0.30 A decaying to -0.02 A.

a universal time basis for the measurements. The output was scaled according to the selected input range and was always inverted. The oscilloscope recorded the absolute voltage at each sense electrode rather than the voltage difference. The internal mathematical algorithm of the oscilloscope was not used to find the voltage difference because it was insufficiently accurate. Rather, this differencing of the two voltage measurements was accomplished with a simple math utility written expressly for this investigation. All data collected by the oscilloscope were recorded in binary on a floppy diskette.

A typical experiment began by setting temperature and waiting for the melt to reach thermal equilibrium. Then the cell was polarized to an applied potential of 0 V versus open circuit for 1–2 min, followed by 0.1 V[9] versus reference for 2 min, and ending with 0 V versus open circuit for 2 min. Fig. 1 shows the current response for the TiO_2–BaO (73:27) melt at a temperature of 1400°C. The oscilloscope monitored the melt voltage, the total current, and the applied voltage at a rate of five samples per second for a total of 500 s. To assure electronic homogeneity after polarization, the cell was subjected to excitation by a triangular waveform between successive square waves. This procedure was repeated at each temperature. At the conclusion of the experiment the electrodes and thermocouple were removed from the melt. The temperature in the furnace was increased to induce the melt to drain from the electrodes. Finally, the furnace was turned off and the melt was cooled to room temperature under flowing argon. It was impossible to remove the hardened melt by chemical means. Hence, each experiment required a new crucible and set of electrodes.[10]

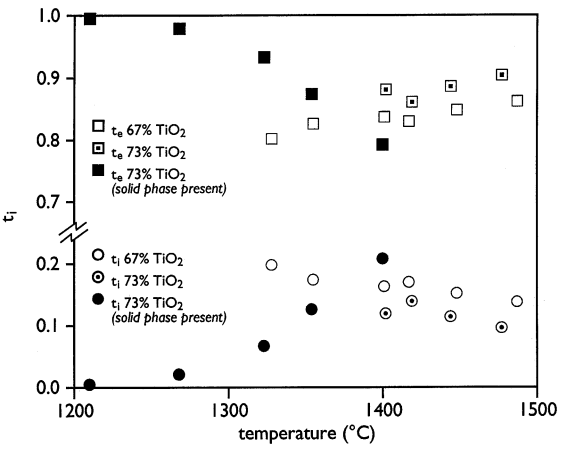

Fig. 2. Temperature dependence of ionic and electronic transference numbers.

5. Results

The technique used in the present investigation allowed the determination of the electronic transference number, t_e, which represents the fraction of total current borne by all electronically conducting species, and the ionic transference number, t_i, which represents the fraction of the total current borne by all ions. As shown above in Eqs. (7)–(16), these can be determined from the current response to a square-wave potential. The value of the initial peak current, denoted $I_{o,\,field}$, is proportional to total melt conductivity. At long times, the only current flowing, denoted $I_{\infty,\,field}$, is that due to electronic conduction. The ratio of the two currents is a measure of t_e

$$t_e = I_{\infty,\,field}/I_{o,\,field} \tag{17}$$

where the subscript, field, indicates that the current is measured while the cell is subjected to an applied potential.

The ionic transference number can be expressed as the ratio of the difference between the current flowing at long times and the initial current

$$t_{i,\,field} = (I_{o,\,field} - I_{\infty,\,field})/I_{o,\,field} \tag{18}$$

As shown in Fig. 1 which is representative of the data, at long times the melt exhibited a non-zero current which is characteristic of electronic conduction. Furthermore, the removal of the square-wave potential

[9] For the barium titanate melt, TiO_2–BaO (73:27), it was necessary to limit the applied potential to ± 0.08 V. Higher voltages caused overloads in the potentiostat's ammeter.

[10] It was possible to reuse the thermocouple thanks to removal of hardened bath by careful grinding.

resulted in a non-zero relaxation current which is characteristic of ionic conduction. Clearly, these melts are mixed conductors.

Fig. 2 shows a plot of the temperature dependence of the ionic and electronic transference numbers of two solutions in the TiO_2–BaO system. For both compositions, in the liquid state the electronic transference number increased linearly with temperature, while the ionic transference number decreased correspondingly.

For TiO_2–BaO (73:27), measurements were made also below the liquidus temperature where it was found that the electronic transference number decreased linearly with temperature, in contrast to its behavior in the molten state. In the all-solid $BaTi_2O_5$–$BaTi_3O_7$ phase field, very high values of t_e were measured (0.995 at 1210°C). In the two-phase fields bounded by liquid, namely, $BaTi_3O_7$–liquid (1317–1357°C) and $BaTi_4O_9$–liquid (1357–1400°C), we measure values of t_e consistent with what one would expect for t_e of the liquid phase present. Since in all cases on this temperature interval the equilibrium liquid phase is at a lower TiO_2 concentration than the mixture and, as we have seen above, t_e scales with TiO_2 concentration, it is reasonable to expect the value of t_e to decrease as temperature increases through these liquid–solid two-phase regimes.

6. Discussion

The electrical properties of these melts are consistent with mixed ionic and semiconducting behavior. Separate measurements indicate that the temperature dependence of the electrical conductivity is well represented by $\ln \sigma T$ versus $1/T$ and that the activation energy is on the order of 0.15 eV [17]. The data reported here show that the ionic conductivity increases with barium concentration which is reasonable given the expected melt speciation (Ba^{2+} and various TiO_x^{n-} moieties). We further expect that TiO_2 is responsible for the semiconducting character of these melts. It is well known that titanium is aliovalent in these systems. The presence of multiple oxidation states facilitates electronic conduction by electron hopping.

As for the question of whether such melts might prove useful as electrolytes for the electrolytic extraction of titanium metal, the present study indicates that it is indeed possible to make major changes in ionicity by altering composition. For example, at 1400°C the ionic transference number, which for all intents and purposes here is the transference number of Ba^{2+}, rises from 0.106 to 0.167 when the BaO concentration is increased from 27 to 33 mol%. Clearly, the ionic transference number needs to be much higher than 0.167 if an electrolysis process is to operate at commercially viable current efficiencies. Unfortunately, limitations in the capabilities of our furnace prevented us from exploring a wider range of composition. Just the same, we believe that this work demonstrates the feasibility of reducing the level of electronic conduction by diluting TiO_2 in an ionic solvent such as BaO.

Acknowledgements

This work was funded principally by the Office of Naval Research (N0000014-90-J1721). The authors thank Dr George Yoder of ONR for his support. Additional funding in the form of graduate research fellowships (for N.A.F.) came from the following: the Ida Greene Fellowship at MIT, the National Defense Science and Engineering Graduate Fellowship through the ONR, the V. Kann Rasmussen Foundation, the Massachusetts Space Grant Consortium Fellowship, the GE Foundation Faculty for the Future Program, the MIT Mining and Minerals Resources Research Institute, and the American Association of University Women Engineering Fellowship. Helpful discussions with Professors Uday B. Pal and Harry L. Tuller are gratefully acknowledged.

References

[1] D.R. Sadoway, J. Mater. Res. 10 (1995) 487.
[2] D.R. Sadoway, J. Metals 43 (7) (1991) 15.
[3] A. Grau, D. Poggi, Can. Metall. Q. 17 (1978) 97.
[4] S.I. Denisov, V.S. Degtyarev, V.A. Reznichenko, Izv. Akad. Nauk SSSR Metal. 1970 (1), 80.
[5] S.A. Klinchikov, E.F. Kustov, T.K. Maketov, G. Steczko, Cryst. Res. Technol. 16 (1) (1981) K21.
[6] V.I. Musikhin, V.M. Lepinskikh, Yu.A. Fomichev, Tr. Inst. Met. Sverdlovsk. 18 (1969) 293.
[7] I.I. Olsen, R. Koksbang, E. Skou, Electrochim. Acta 40 (1995) 1701.
[8] J. Evans, C.A. Vincent, P.G. Bruce, Polymer 28 (1987) 2324.
[9] P.G. Bruce, C.A. Vincent, J. Electroanal. Chem. Interfacial Electrochem. 225 (1987) 1.
[10] P.G. Bruce, J. Evans, C.A. Vincent, Solid State Ionics 28/30 (1988) 918.
[11] Y.C. Yeh, T.Y. Tseng, D.A. Chang, J. Am. Ceram. Soc. 73 (7) (1990) 1992.
[12] S. Colson, S.P. Szu, L.C. Klein, J.M. Tarascon, Solid State Ionics 46 (3–4) (1991) 283.
[13] M. Watanabe, M. Togo, K. Sanui, N. Ogata, T. Kobayashi, Z. Ohtaki, Macromolecules 17 (1984) 2908.
[14] O.A. Esin, A.I. Sotnikov, Yu.P. Nikitin, Dokl. Akad. Nauk SSSR 158 (1964) 1149.
[15] D.E. Rase, R. Roy, J. Am. Ceram. Soc. 38 (1955) 102.
[16] S.L. Schiefelbein, N.A. Fried, K.G. Rhoads, D.R. Sadoway, Rev. Sci. Instrum. 69 (9) (1998) 3308.
[17] N.A. Fried, PhD thesis, Massachusetts Institute of Technology, Cambridge, MA, 1996.